

Photophysical properties of quinoxaline-fused [7]carbohelicene derivatives

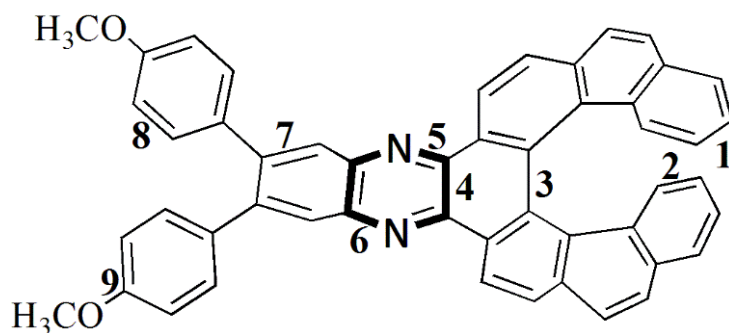
Chunyu Liu,^a Yanling Si,^b Xiumei Pan^{a,*} and Guochun Yang^{a,*}

- a. Institute of Functional Material Chemistry, Faculty of Chemistry, Northeast Normal University, Changchun
130024 Jilin, China.
E-mail: yanggc468@nenu.edu.cn
- b. College of Resource and Environmental Science, Jilin Agricultural University,
Changchun, 130118 Jilin, China

Contents

1. The main concerned bond length for compound **4** between experiment and calculation. **S3**
2. Computed absorption wavelengths (nm) using the B3LYP functional at the different basis sets level for compound **2**. **S4**
3. Calculated UV-Vis (left) and CD (right) spectra of compound **2** using six different DFT functionals. **S5**
4. Computed HOMO and LUMO energy level and corresponding energy gaps ($E_g=LUMO-HOMO$) in eV using different functionals at 6-31+G(d) basis set level for compound **2**. **S6**
5. The calculated excitation energies, oscillator strengths and rotational strengths for compound **2** in the gas phase at the TDB3LYP/ 6-31+G(d) level. **S7**
6. Computed absorption wavelengths (λ in nm), oscillator strengths (f), and major contribution for the studied compounds **1, 3, 4, 5** and **6**. **S9**
7. Calculated UV-Vis (left) and CD (right) spectra in solution phases(THF) of **1** and **3** at the TDB3LYP/6-31+G(d) level of theory along with gas phases UV-Vis and CD (red dash line). **S10**
8. Molecular orbital isosurfaces involved in the main electron transitions of compounds **1, 3, 4** and **6** at the TDB3LYP/6-31+G(d) level of theory. **S11**
9. Computed HOMO and LUMO energy level and corresponding energy gaps (E_g) in eV at the TDB3LYP/6-31G(d,p) level for compounds **1-6**. **S13**
10. Molecular orbitals involved into the main CD transition of compounds **1-4**. **S14**
11. Calculated band structure of the crystal for compound **4** in its racemate (top) and enantiomer crystals (bottom). **S16**

Table S1. The main concerned bond length for compound **4** between experiment and calculation.



Bond	B3LYP	Experiment	Difference
1	1.407	1.405	0.002
2	1.382	1.379	0.003
3	1.479	1.479	0.000
4	1.439	1.438	0.001
5	1.330	1.333	-0.003
6	1.352	1.355	-0.003
7	1.383	1.369	0.014
8	1.397	1.377	0.020
9	1.365	1.370	0.005

Note: the difference is equal to calculation value minus experimental value

Table S2. Computed absorption wavelengths (nm) using the B3LYP functional at the different basis sets level for compound **2** along with the experimental values.

Basis set	Band 1	Band 2	Band 3	Band 4
6-31G(d)	278.90	313.25	341.40	419.99
6-31+G(d)	282.49	316.45	346.13	424.85
6-31++G(d,p)	282.74	316.54	346.24	424.78
6-311++G(d,p)	283.80	317.94	348.20	426.72
6-311++G(2d,2p)	284.42	318.48	349.18	427.27
exp	276	332	366	427

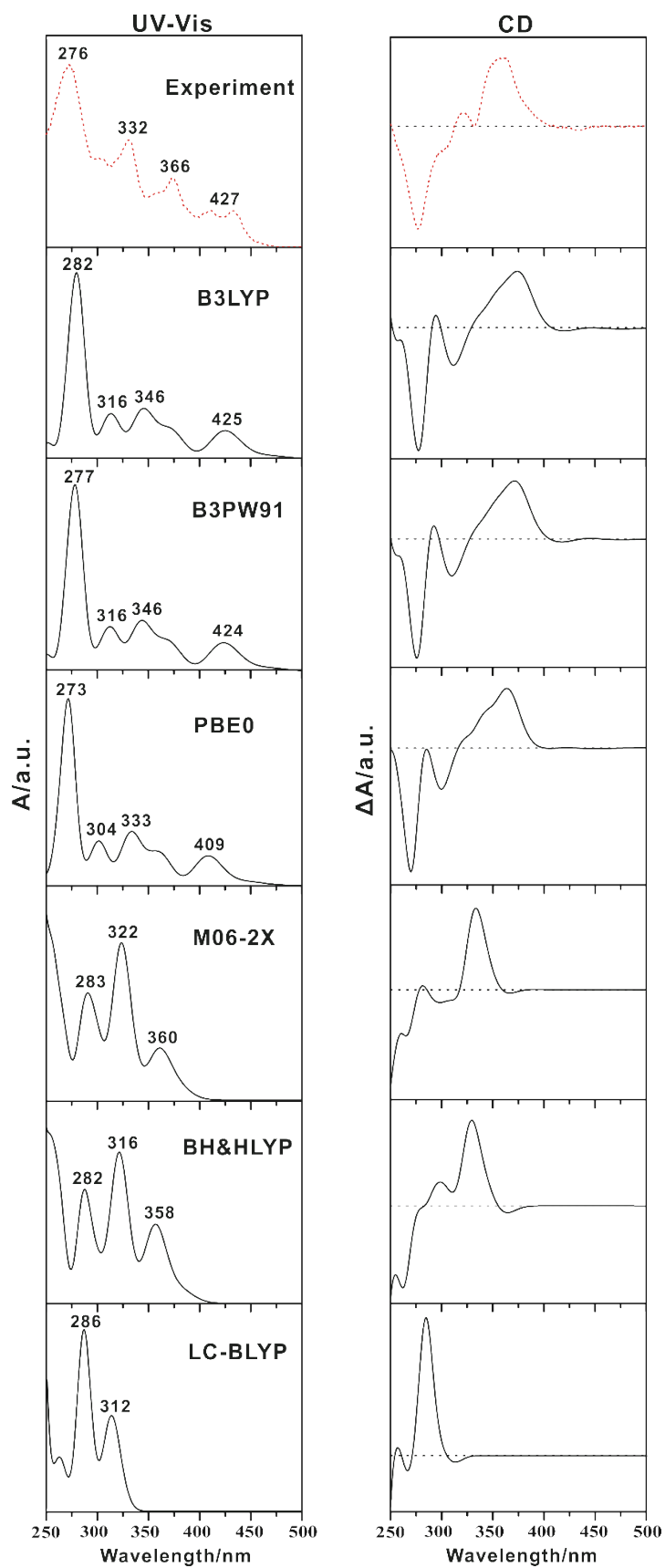


Figure S1. Calculated UV-Vis (left) and CD (right) spectra of compound **2** using six different DFT functionals along with the experimental spectra.

Table S3. Computed HOMO and LUMO energy level and corresponding energy gaps (E_g =LUMO-HOMO) in eV using different functionals at 6-31+G(d) basis set level for compound **2**.

Functional	HUMO	LUMO	E_g
B3LYP	-5.757	-2.574	3.183
PBE0	-5.961	-2.480	3.481
B3PW91	-5.819	-2.628	3.191
M06-2X	-6.896	-1.835	5.061
BH&HLYP	-6.537	-1.603	4.934
LC-BLYP	-8.226	-0.481	7.745

Table S4. The calculated excitation energies, oscillator strengths and rotational strengths for compound **2** in the gas phase at the TDB3LYP/ 6-31+G(d) level.

states	eV	λ^a	f^b	Rlength ^c	Rvelocity ^c
1	2.6440	468.92	0.0224	5.5739	5.1048
2	2.8851	429.74	0.0112	-46.2693	-45.2348
3	2.9183	424.85	0.1891	57.2984	54.9835
4	3.2810	377.88	0.0005	-0.0633	-0.2286
5	3.2991	375.81	0.0674	-308.9714	-309.9281
6	3.3071	374.90	0.0693	53.0994	52.4732
7	3.3946	365.23	0.0832	-3.5566	-3.5030
8	3.4951	354.74	0.0076	-126.4121	-124.9949
9	3.5685	347.44	0.0692	-191.9522	-191.1530
10	3.5820	346.13	0.2068	211.4651	205.9730
11	3.6540	339.31	0.0080	-46.5211	-43.4195
12	3.6855	336.41	0.0844	-28.7331	-28.0954
13	3.9180	316.45	0.2195	59.3692	57.4197
14	4.0151	308.79	0.0742	78.5611	75.1716
15	4.0341	307.34	0.0435	57.8225	57.9084
16	4.0579	305.54	0.0247	-15.2280	-15.2438
17	4.1594	298.08	0.0038	-10.5911	-9.6629
18	4.1642	297.74	0.0044	10.5572	10.8161
19	4.2477	291.88	0.0157	-22.4081	-22.3610
20	4.2734	290.13	0.0164	-78.0292	-77.1421
21	4.3173	287.18	0.0047	-1.8169	-2.0775
22	4.3442	285.40	0.0326	-136.8769	-133.1782
23	4.3890	282.49	0.7815	259.6704	254.5679
24	4.4281	280.00	0.0078	4.4532	4.0056
25	4.4535	278.40	0.3126	298.5076	292.8781
26	4.4936	275.91	0.0988	-119.4684	-112.3997
27	4.5204	274.28	0.0349	30.4146	30.5501
28	4.5659	271.54	0.3065	229.5874	220.4800
29	4.5846	270.44	0.0369	-9.2351	-8.3509
30	4.7298	262.14	0.0010	-18.0344	-19.9286
31	4.7745	259.68	0.0095	-46.7129	-43.8157
32	4.7990	258.35	0.0031	42.5221	38.4494
33	4.8537	255.44	0.0023	44.1085	44.8482
34	4.8836	253.88	0.0291	4.2786	4.0528
35	4.8861	253.75	0.0209	-5.1898	-4.4951
36	4.9057	252.73	0.0026	31.8721	31.3515
37	4.9553	250.20	0.0466	-14.3257	-13.2494
38	4.9798	248.97	0.0055	-12.4077	-12.0278
39	4.9947	248.23	0.0012	-15.4280	-12.0929

40	5.0903	243.57	0.0200	-110.1612	-106.9509
41	5.1060	242.82	0.0107	-3.9865	-4.1217
42	5.1659	240.00	0.0041	6.5592	6.3127
43	5.1684	239.89	0.0309	-42.0964	-39.9093
44	5.2035	238.27	0.0006	1.7824	1.9336
45	5.2075	238.09	0.0000	-0.1136	-0.0247
46	5.2152	237.73	0.0007	6.3266	4.7656
47	5.2533	236.01	0.0130	31.0118	31.8413
48	5.2641	235.53	0.0003	0.7014	1.2800
49	5.3123	233.39	0.0138	-16.7621	-16.5259
50	5.3147	233.28	0.0012	1.9467	1.7718
51	5.3380	232.27	0.0001	3.3390	3.8701
52	5.3414	232.12	0.0220	-25.3855	-23.4324
53	5.3547	231.54	0.0506	4.6474	4.4342
54	5.3696	230.90	0.0169	39.5927	38.1616
55	5.3933	229.88	0.0010	4.0598	3.9349
56	5.4053	229.37	0.0129	-18.3724	-16.9195
57	5.4072	229.30	0.0052	-22.3822	-21.8288
58	5.4309	228.29	0.0107	-24.7518	-24.4644
59	5.4401	227.91	0.0169	2.4085	2.4843
60	5.4525	227.39	0.1216	-107.9398	-105.0485

^a λ in nm. ^b Oscillator Strengths. ^c R values (in 10^{-40} esu²cm²) using the velocity-gauge representation and length-gauge representation of the electric dipole operator.

Table S5. Computed absorption wavelengths (λ in nm) as compared to experimental data (in parentheses), oscillator strengths (f), and major contribution for the studied compounds **1**, **3**, **4**, **5** and **6**.

Compound	λ	f	Major contribution
1	273.82(272)	0.509	HOMO-1 \rightarrow LUMO+3 (44%) HOMO-3 \rightarrow LUMO (13%)
	311.91(303)	0.015	HOMO-3 \rightarrow LUMO+1 (55%) HOMO-1 \rightarrow LUMO+2 (42%)
	374.34(373)	0.104	HOMO \rightarrow LUMO+1 (59%) HOMO-1 \rightarrow LUMO (25%)
3	272.71(283)	0.366	HOMO-2 \rightarrow LUMO+5 (32%) HOMO-12 \rightarrow LUMO (19%)
	301.46(335)	0.128	HOMO-1 \rightarrow LUMO+3 (44%) HOMO \rightarrow LUMO+5 (15%)
	349.57(378)	0.640	HOMO-2 \rightarrow LUMO+1 (39%) HOMO \rightarrow LUMO+1 (29%)
	438.13(445)	0.416	HOMO-1 \rightarrow LUMO (88%) HOMO \rightarrow LUMO+1 (9%)
4	276.15(286)	0.064	HOMO-12 \rightarrow LUMO (33%) HOMO-8 \rightarrow LUMO+1 (14%)
	308.78(333)	0.251	HOMO-8 \rightarrow LUMO (51%) HOMO-4 \rightarrow LUMO+2 (16%)
	352.72(383)	0.573	HOMO \rightarrow LUMO+2 (51%) HOMO-1 \rightarrow LUMO+1 (22%)
	449.65(450)	0.571	HOMO-1 \rightarrow LUMO (93%)
5	287.72	0.478	HOMO-1 \rightarrow LUMO+5 (48%) HOMO-2 \rightarrow LUMO+4 (15%)
	312.87	0.302	HOMO-8 \rightarrow LUMO (34%) HOMO \rightarrow LUMO+3 (31%)
	359.21	0.579	HOMO-1 \rightarrow LUMO+2 (52%) HOMO \rightarrow LUMO+1 (17%)
	476.34	0.533	HOMO \rightarrow LUMO (96%)
6	285.74	0.408	HOMO \rightarrow LUMO+7 (46%) HOMO-1 \rightarrow LUMO+5 (12%)
	348.46	0.498	HOMO-2 \rightarrow LUMO+3 (57%) HOMO \rightarrow LUMO+3 (14%)
	456.00	0.412	HOMO \rightarrow LUMO+1 (64%) HOMO-1 \rightarrow LUMO (34%)

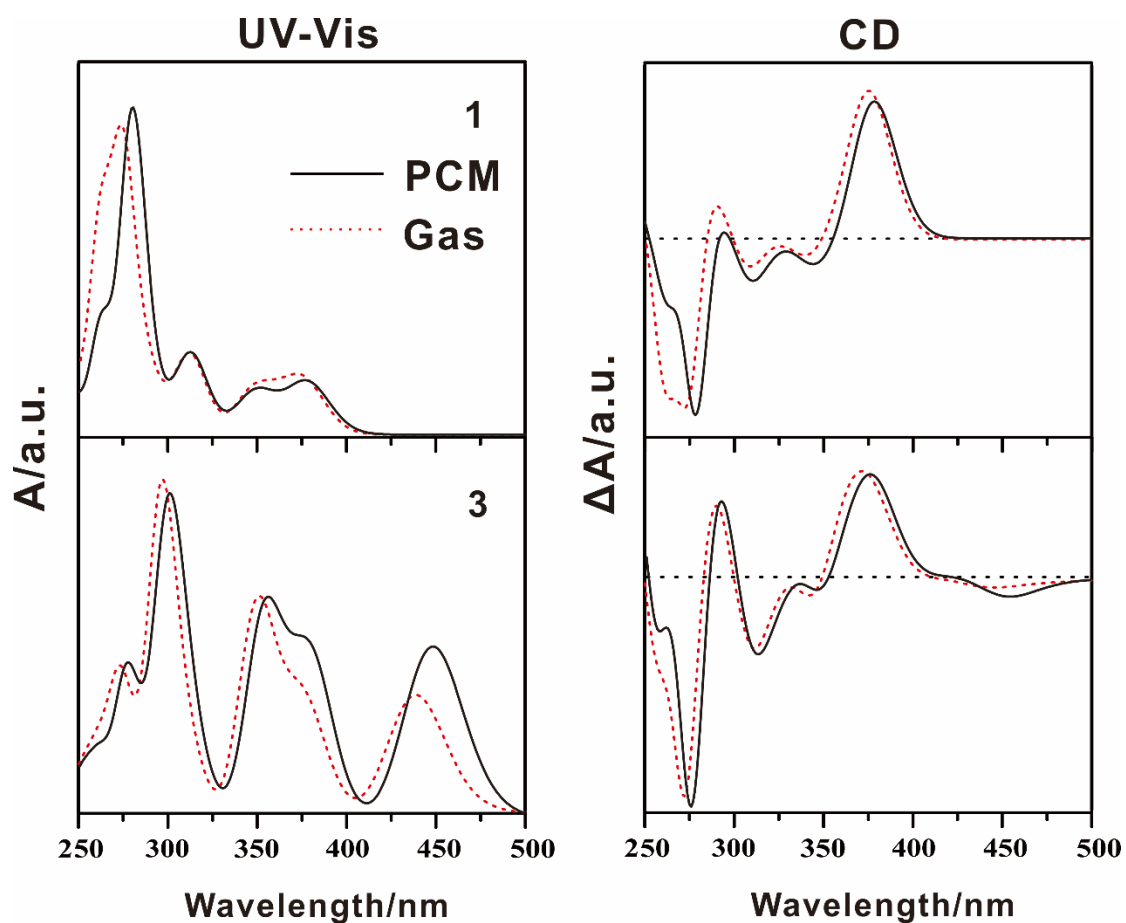
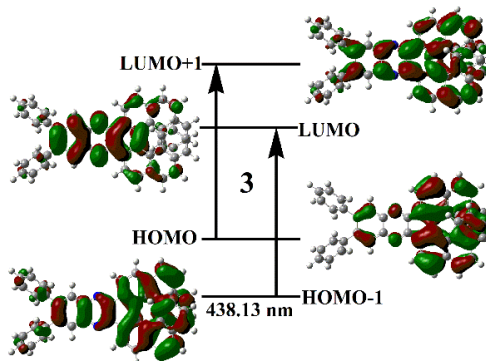
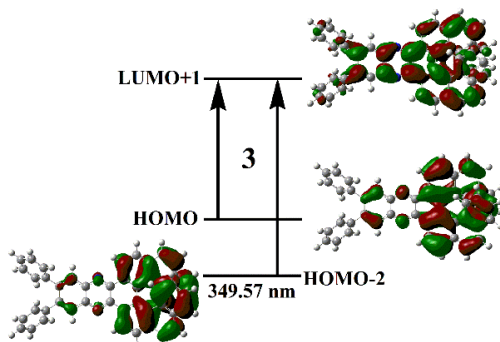
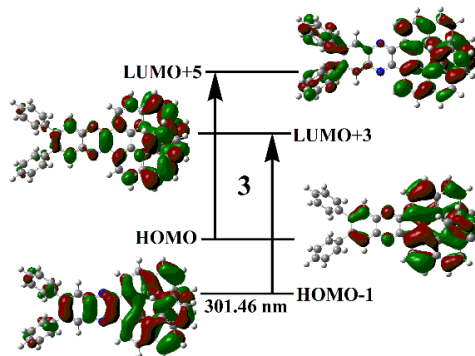
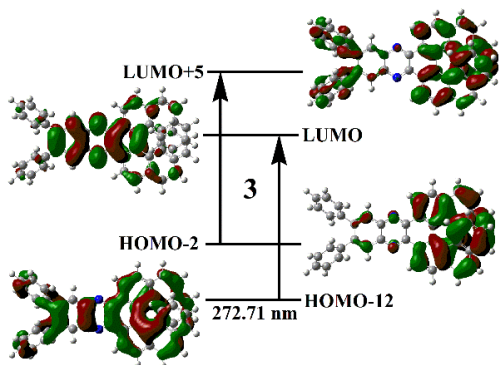
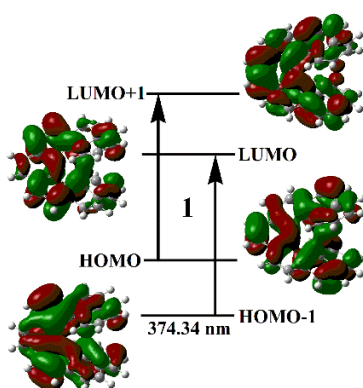
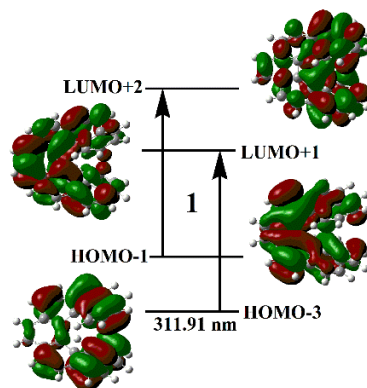
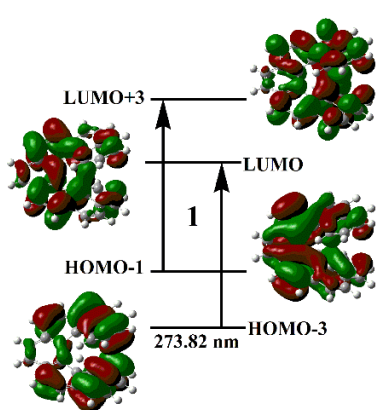


Figure S2. Calculated UV-Vis (left) and CD (right) spectra in solution phases(THF) of **1** and **3** at the TDB3LYP/6-31+G(d) level of theory along with gas phases UV-Vis and CD (red dash line).



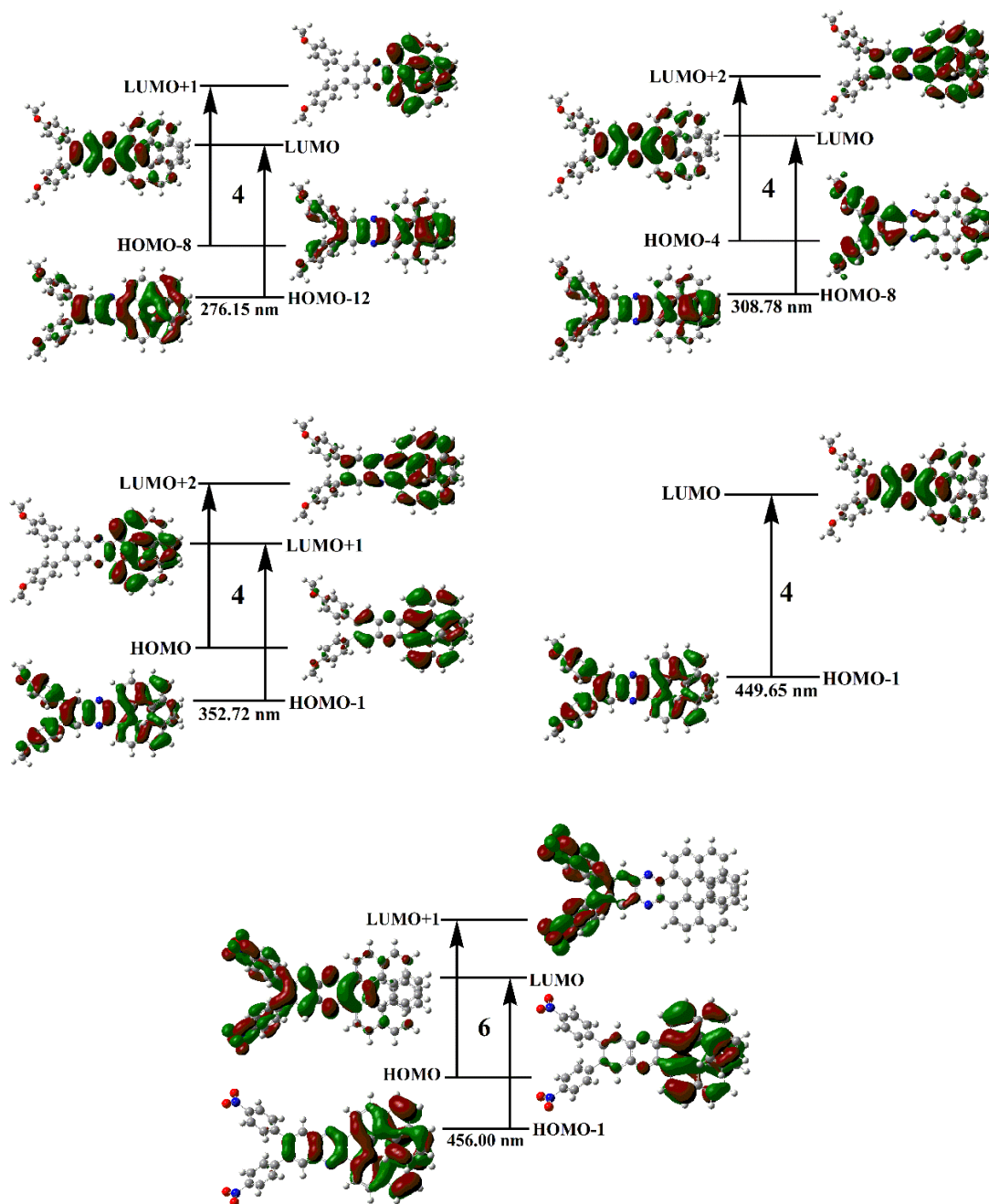
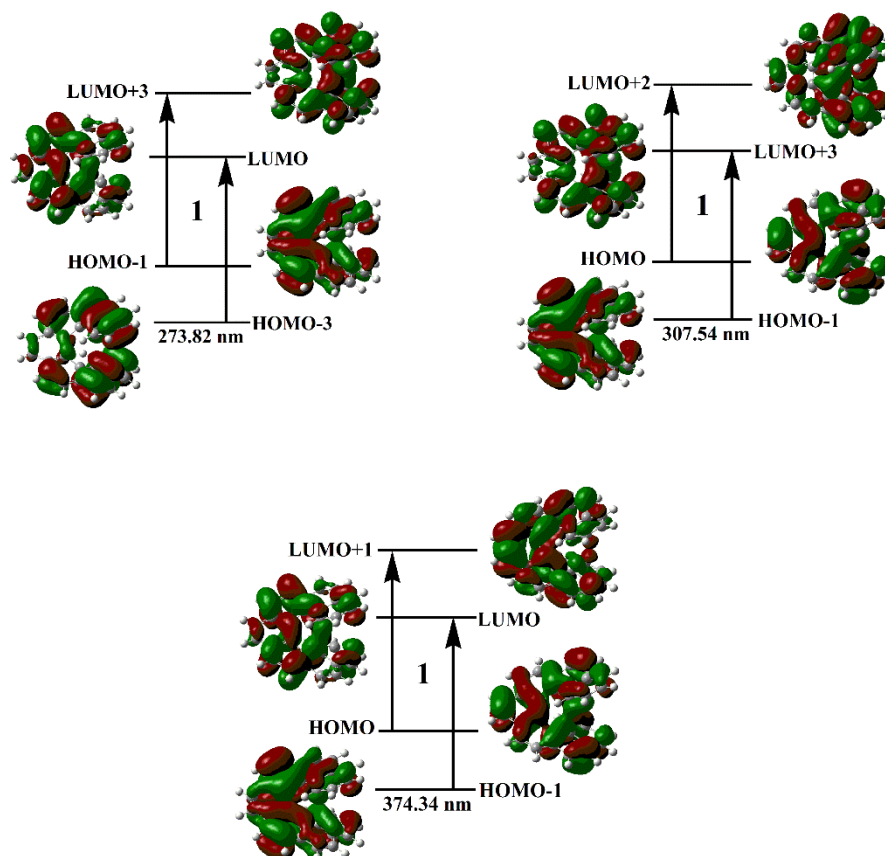


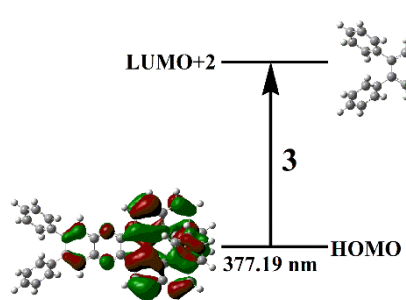
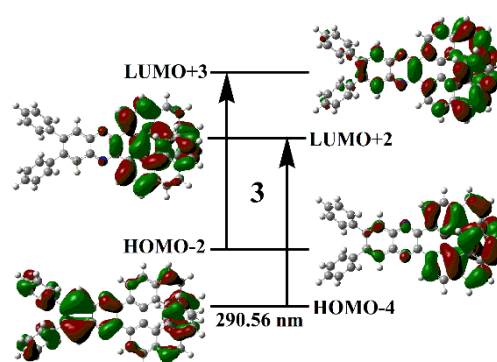
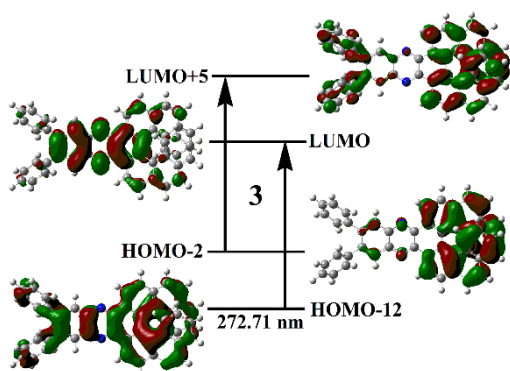
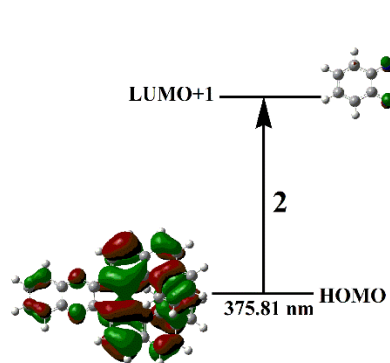
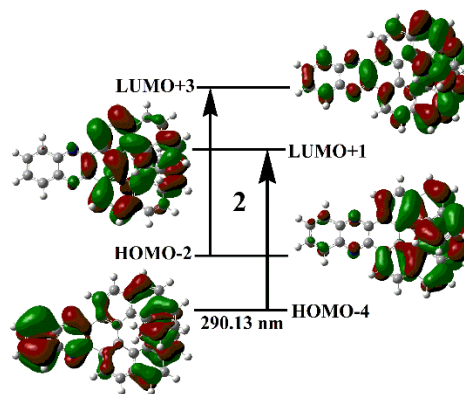
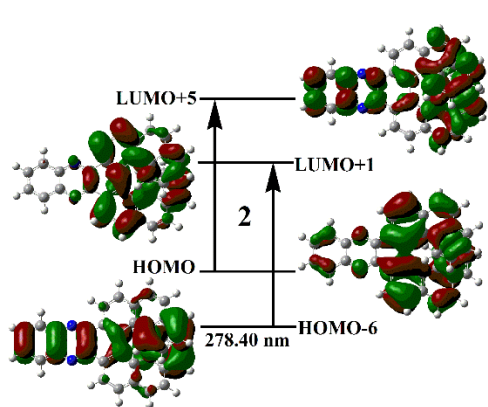
Figure S3. Molecular orbital isosurfaces involved in the main electron transitions of compounds **1**, **3**, **4** and **6** at the TDB3LYP/6-31+G(d) level of theory.

Table S6. Computed HOMO and LUMO energy level and corresponding energy gaps

(E_g =LUMO-HOMO) in eV at the TDB3LYP/6-31G(d,p) level for compounds 1-6.

Compound	HOMO	LUMO	E_g
1	-5.371	-1.508	3.863
2	-5.484	-2.272	3.212
3	-5.454	-2.295	3.159
4	-5.377	-2.198	3.179
5	-5.114	-2.099	3.015
6	-5.767	-2.844	2.923





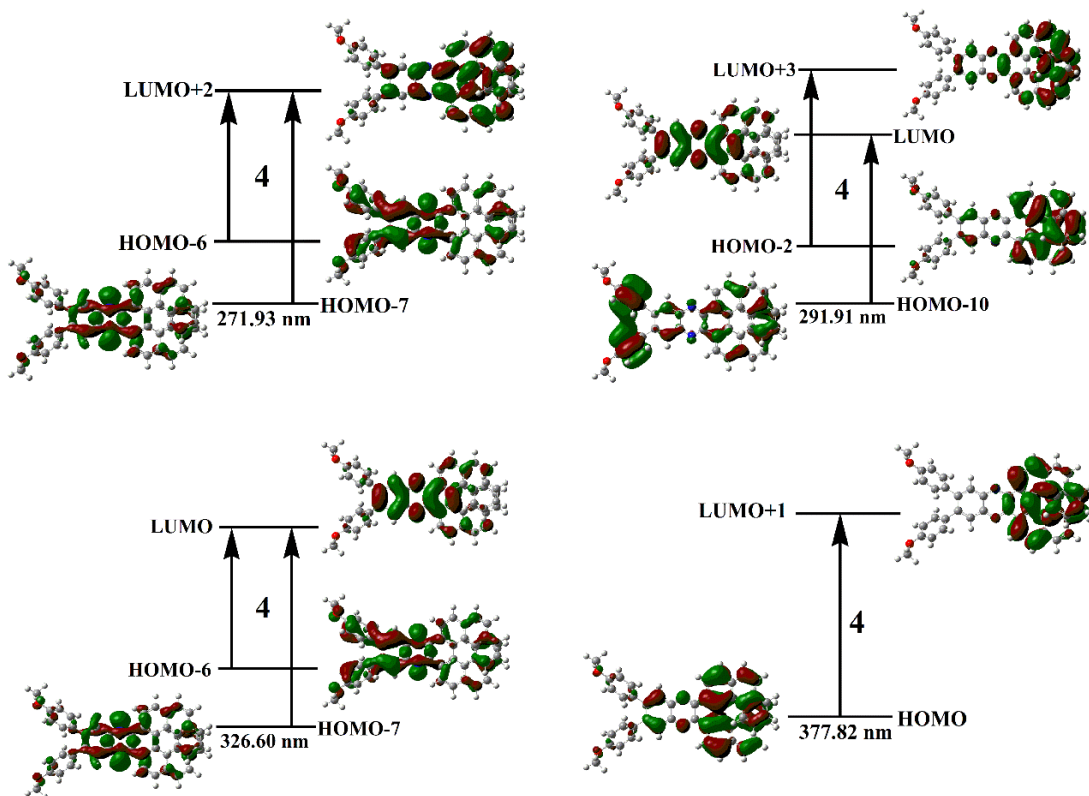
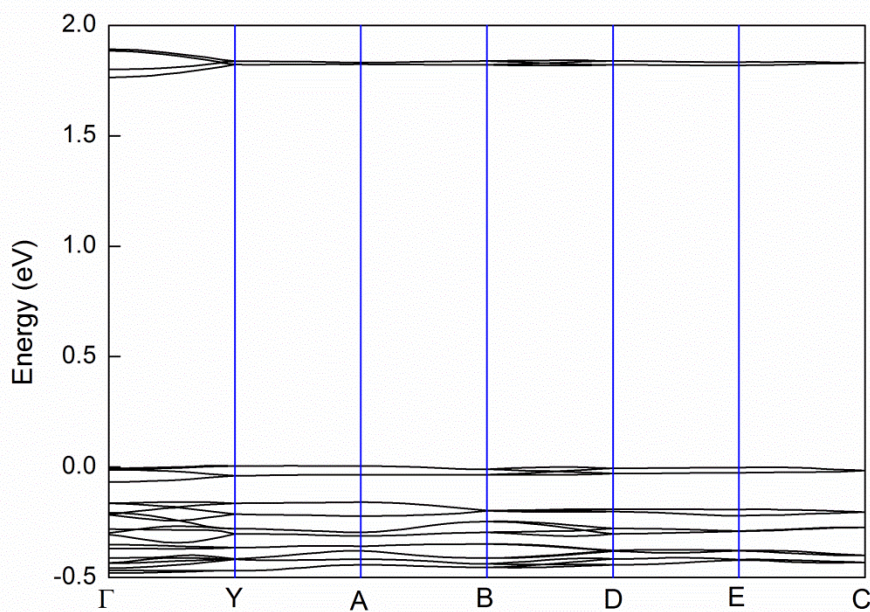


Figure S4. Molecular orbitals involved into the main CD transition of compounds 1-4.



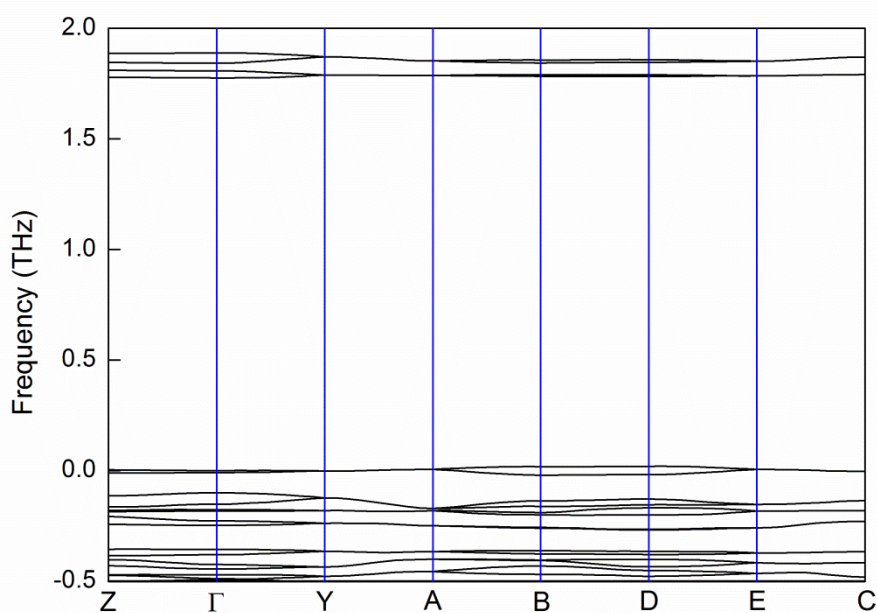


Figure S5. Calculated band structure of the crystal for compound **4** in its racemate (top) and enantiomer crystals (bottom). The high symmetry points in racemate are $\Gamma = (0, 0, 0)$, $Y = (0, 0.5, 0)$, $A = (-0.5, 0.5, 0.5)$, $B = (-0.5, 0, 0)$, $D = (-0.5, 0, 0.5)$, $E = (-0.5, 0.5, 0.5)$ and $X = (0, 0.5, 0.5)$. The high symmetry points in enantiomer crystals are $Z = (0, 0, 0.5)$, $\Gamma = (0, 0, 0)$, $Y = (0, 0.5, 0)$, $A = (-0.5, 0.5, 0.5)$, $B = (-0.5, 0, 0)$, $D = (-0.5, 0, 0.5)$, $E = (-0.5, 0.5, 0.5)$ and $X = (0, 0.5, 0.5)$.